Food & Function

The viability of complex coacervates encapsulated probiotics during simulated sequential gastrointestinal digestion as affected by wall materials and drying methods

Journal:	*Food & Function*
Manuscript ID	FO-ART-05-2021-001533.R1
Article Type:	Paper
Date Submitted by the Author:	16-Jun-2021
Complete List of Authors:	Qi, Xiaoxi; North Dakota State University, plant sciences Lan, Yang; North Dakota State University, Plant Sciences Ohm, Jae-Bom; USDA-ARS Northern Plains Area, , Red River Valley Agricultural Research Center, Cereal Crops Research Unit, Hard Spring and Durum Wheat Quality Lab Chen, Bingcan; North Dakota State University, Plant Sciences Rao, Jiajia; North Dakota State University, Plant Sciences

The viability of complex coacervates encapsulated probiotics during simulated sequential gastrointestinal digestion as affected by wall materials and drying methods

Xiaoxi Qi[1], Yang Lan[1], Jae-Bom Ohm[2], Bingcan Chen[1], Jiajia Rao[1*]

1. Food Ingredients and Biopolymers Laboratory, Department of Plant Sciences, North Dakota State University, Fargo, ND 58102, USA

2. USDA-ARS, Red River Valley Agricultural Research Center, Cereal Crops Research Unit, Hard Spring and Durum Wheat Quality Lab., Fargo, ND 58108, USA

Submission Journal: Food & Function

Resubmission Date: June, 2021

*To whom correspondence should be addressed. Tel: 1 (701) 231-6277. Fax: 1 (701) 231-7723. E-mail: Jiajia.rao@ndsu.edu.

Abstract

The objective of this study was to investigate the impact of protein type (sodium caseinate and pea protein isolate), protein to sugar beet pectin mixing ratio (5:1 and 2:1) on complex coacervation formation, as well as the impact of the finishing technology (freeze-drying and spray-drying) for improving the viability of encapsulated *Lactobacillus rhamnosus GG* (LGG) in the complex coacervates during simulated sequential gastrointestinal (GI) digestion. The physicochemical properties of LGG encapsulated microcapsules in liquid and powder form were evaluated. The state diagram and ζ-potential results indicated that pH 3.0 was the optimum pH for coacervates formation pH in the current systems. Confocal laser scanning microscopy (CLSM), viscoelastic analysis, and Fourier transform infrared spectroscopy (FTIR) confirmed that the gel-like network structure of complex coacervates were successfully formed between protein and SBP at pH 3.0 through electrostatic interaction. In terms of physiochemical properties and viability of LGG encapsulated in the microcapsules powder, drying method played a crucial role on particle size, microstructure and death rate of encapsulated LGG during simulated sequential GI digestion compared to protein type and biopolymer mixing ratio. For example, the microstructure of spray-dried microcapsules exhibited smaller spherical particles with some cavities, whereas the larger particle size of freeze-dried samples showed porous sponge network structure with larger particle sizes. As a result, spray-dried LGG microcapsules generally had a lower death rate during simulated sequential gastrointestinal digestion compared to the freeze-dried counterpart. Among all samples, spray-dried PPI–SBP microcapsules demonstrated superior performance against cell loss and maintained more than 7.5 Log CFU/g viable cells after digestion.

Key words: complex coacervates; protein type, spray-drying, freeze-drying, viability, probiotics

1. Introduction

Probiotics are living microorganisms that can confer the host with numerous health benefits. A number of probiotics like *Lactobacillus* and *Bifidobacterium*, as well as some other species such as *Escherichia*, *Saccharomyces*, *Bacillus*, *Streptococcus* have been applied in a wide range of functional foods, beverages, supplements, and pharmaceuticals [1]. However, these potential health benefits offered by the probiotics can only be achieved if sufficient numbers of live cells are maintained after passing through the human gastrointestinal (GI) tract. The common consensus of attaining these benefits is that the number of probiotics should be no less than 10^6 viable cells per dose/day for supplement at the time of consumption [2]. Nevertheless, majority of the probiotics have remarkable loss of their viability after they pass through the GI tract because of their poor tolerance of low pH at stomach and high bile salt concentration in small intestine. As such, various encapsulation techniques have been explored for improving the viability of the probiotics during GI tract [3].

Among most of the techniques, complex coacervation is an unique and promising encapsulation techniques to protect bioactive compounds due to its mild processing conditions, controlled release, as well as good acidic tolerance [4]. In general, complex coacervation is an associative phase separation phenomenon originated from electrostatic attraction between two oppositely charged biopolymers [5]. Depending on the strength of electrostatic attraction, the biopolymer mixture can be separated into solvent-rich phase and biopolymer-rich phase. The biopolymer rich phase is a gel-like structure that can be applied as wall materials for encapsulating probiotics. Previous studies have proved that complex coacervates have a favorable impact on improving the viability of the encapsulated probiotics [6-8]. The typical procedure of forming probiotics encapsulated in complex coacervation starts from mixing of

probiotics with protein–polysaccharide solution at a proper mass ratio, followed by the adjustment of pH of this ternary mixture to a certain pH to induce phase separations between the biopolymers and solution. At last, the liquid probiotics encapsulated by means of complex coacervates can be turned into powder form through drying processing. The physical properties of complex coacervates are dependent of several factors, such as wall material compositions, the mass ratio between protein–polysaccharide, and optimum complex coacervates formation pH [9]. These factors also determine the functional performance of complex coacervates as a microencapsulation wall material for protecting the viability of probiotics under harsh conditions.

Most of the current existing complex coacervation systems are formed from animal based proteins, such as gelatin, sodium caseinate (SC) and whey protein [10, 11]. Among them, SC seemed to have advantages of protecting probiotics during thermal processing and GI tract because of its more hydrophobic and higher thermal stability properties [12]. On the other hand, the trend on fabrication of pea protein-based complex coacervates to be as microencapsulation vehicles is on a quick rise due to the emerging usages of plant-based ingredients in food systems. Based on the previously reported studies, pea protein is able to from complex coacervates with various polysaccharides and maintain decent functionalities, [13, 14]. Hence, involving pea protein as microencapsulation vehicles instead of the traditional animal proteins in complex coacervation is another path to improve the viability of the encapsulated probiotics. However, the protective effects of pea protein-based complex coacervates as capsule materials on the encapsulated probiotics has yet to be explored.

Upon formation of complex coacervates encapsulated probiotics, drying is the last step to develop commercially available probiotics functional foods. In general, spray-drying and freeze-

drying are the two most common methods for drying microcapsules of probiotics, with which different microstructure is formed [15]. Freeze-drying is a mild technology for protecting viability of probiotics during drying processing; it, however, cannot efficiently reduce the particle size of microcapsules as compared to spray-drying. To date, there are few studies which focus on the drying methods on viability and functionality of probiotics [16]. Consequently, it is necessary to take drying processing in combination of complex coacervates formula into account on the viability of probiotics.

This study was aimed to gain more insights into how protein type and drying processing influence the physicochemical properties of complex coacervates and the protective effects on probiotics. Two different proteins (SC and pea protein isolate) were selected to form complex coacervates with sugar beet pectin (SBP) to improve the viability of a well-studied probiotic strain, *Lactobacillus rhamnosus* GG (LGG) during simulated sequential GI digestion. Besides, considering the application of complex coacervates in food systems, two different drying methods (i.e. spray-drying and freeze-drying) were employed to transform gel-like complex coacervates to powder form and to compare their impact on the viability of probiotics. Therefore, this investigation was undertaken to i) optimize the complex coacervates formation pH between protein–SBP at different mixing ratios, ii) characterize the physicochemical properties of LGG encapsulated microcapsules by means of complex coacervates, and iii) compare different proteins and drying methods on the improvement of the viability of encapsulated LGG during GI tract.

2. Materials and Methods

2.1. Materials

Freeze-dried pea protein isolate (PPI) was extracted from yellow pea flour by alkali extraction-isoelectric precipitated method, as described by [9] without any modification. The final PPI powder contains 79.50% protein (wet basis, %N × 6.25) according to the results obtained from LECO combustion analyzer (St. Joseph, MI). Sugar beet pectin (SBP) (Betapec RU301, Lot # 11710767, 45 kDa of Mw, 55% of degree of esterification (DE), 65% of galacturonic acid, as reported by the manufacturer) was kindly donated by Herbstreith & Fox KG (Neuenbürg, Germany) and used without any purification. Sodium caseinate (SC) from bovine milk (C8654, Lot # SLBS5159), potassium phosphate monobasic, and potassium phosphate monobasic were purchased from Sigma-Aldrich (St. Louis, MO, USA). CRITERION™ Lactobacilli MRS broth was purchased from Hardy Diagnostics (Santa Maria, CA, USA). MRS agar and the multi-use sachets with indicator for creating anaerobic atmosphere were obtained from BD (Franklin Lakes, NJ, USA). Other chemicals and reagents used in this study were of analytical grade and purchased from VWR (Chicago, Illinois, USA). All solutions were prepared using ultrapure distilled de-ionized water (DDW, 18.2 MΩ cm) by the Barnstead Nanopure ultrapure water system (Thermo Scientific, Waltham, MA, USA).

2.2. Optimization of pH condition for complex coacervates formation

2.2.1. Preparation of biopolymer stock solutions

Both PPI (2.0 wt%) and SBP stock solutions (2.0 wt%) were prepared according to our previous published procedure without any modification [14]. SC stock solution (2.0 wt%) was prepared by dispersing SC into 10 mM phosphate buffer (pH 7.0) and stirred at 500 rpm for 12 h at 25 °C, and then adjusted to pH 7.0 using 0.1 M NaOH.

2.2.2. Preparation of biopolymer mixtures

The protein concentration was fixed at 1.0 wt% and the SBP concentration was varied to achieve the initial protein–SBP ratio at 5:1 and 2:1. The pH of biopolymer mixture was then adjusted from 5.0 to 2.5 with 0.5 decrement by the addition of HCl.

2.2.3. Optimizing the pH condition for complex coacervation between protein and SBP

2.2.3.1 Construction of state diagram

The biopolymer mixtures prepared in section 2.2.2 were left to stand static for 24h at 4°C to allow phase separation, the state diagram of protein–SBP mixtures and pure proteins was constructed based on visual observation as stated by Lan et al. [9]. Three different symbols were applied to describe different phase behaviors of the observed phase separations in the test tubes; they were □, ▲, and ■ which represented turbid solution, precipitation & cloudy solution, and precipitation & clear solution, respectively.

2.2.3.2 Surface charge analysis

Surface charges of single biopolymer solutions (1.0 wt% SC, PPI, and SBP) and protein–SBP mixtures were measured using a Zetasizer Nano-ZS 90 (Malvern Instruments, Worcestershire, UK), and reported as zeta-potential (ζ, mV).

2.3. Encapsulation of probiotics in protein-SBP complex coacervates

LGG bacterial cells were cultured in MRS broth at 37 °C under anaerobic condition. After second revival of this strain in MRS broth, the bacterial pellet was obtained by centrifugation at 3,500 rpm for 10 min at 4 °C and washed twice by ultrapure water. The pellet was weighed and added to biopolymer mixture at a total biopolymer solid: bacteria ratio of 2:1 (by weight). The final uniform probiotics biopolymer suspension contained approximately 8.5–9.2 Log CFU/mL cells. According to the optimized conditions (section 2.2.3), the pH of the

probiotics biopolymer suspension was adjusted to 3.0 using 0.1–2.0 M NaOH to promote complex coacervation between protein and SBP, and left for 1h at 4°C. The viscoelastic and microstructure properties of wet microcapsules were then characterized (section 2.4).

2.4. Viscoelastic and microstructure properties of wet microcapsules

Wet microcapsules were first centrifuged at 2,000 rpm for 10 min using Sorvall™ biofuge primo benchtop centrifuge (Thermo Scientific Inc., MA, USA), and precipitates were collected. The dynamic viscoelastic properties of precipitates were evaluated using a Discovery Hybrid Rheometer-2 rheometer (TA Instruments Ltd., New Castle, DE, USA) described by Lan et al [14] with no modification.

LSM 700 confocal laser scanning microscope (CLSM) (Carl Zeiss Microscopy Ltd., Jena, Germany) was applied to investigate the microstructure of the wet microcapsules by following a previously reported method (Chen, Li, Ding, & Suo, 2012) with some modifications. In brief, rhodamine B (50 mg/L), the dye to stain proteins, was prepared by dissolving it in water. Subsequently, 2.0 mL of the wet microcapsules were mixed with 20 μL rhodamine B (50 mg/L) in a test tube and vortexed for 2 min. Afterwards, 200 μL of the stained mixture was placed on a μ-plate 96 well (ibidi USA, Inc., WI, USA), and then the shape and size of rhodamine B-labeled protein–SBP complex coacervates were observed under CLSM using excitation wavelength of 555 nm and emission wavelength of 630 nm.

2.5. Preparation of microcapsule powders by different drying methods

In total, eight microcapsules encapsulated probiotics powders were produced by either spray-drying or freeze-drying. **Table S-1** listed the formulations and codes of eight microcapsule powders prepared in this study. Spray-dried samples were obtained by feeding liquid sample into a Büchi mini spray-dryer B-290 (New Castle, DE, USA) with feed rate of 0.15 L/h and aspirator

flow of 40 L/h. The inlet and outlet air temperature were maintained at 130°C and 55°C, respectively. Regarding freeze-drying process, liquid samples were first frozen in -80 ℃ freezer for 2h, then placed in a foil plate and lyophilized using a SP scientific Lyophilizer (Gardiner, NY, USA) for 24h. The freeze-dried microcapsules were ground into uniform powder with mortar and pestle. Eight microcapsule powders were collected and stored in glass bottles at 4°C for further characterization.

2.6. Characterization of microcapsules powders

IR spectra of microcapsule powders and individual biopolymer powders (SC, PPI, and SBP) were acquired by a Varian FTIR spectrophotometer (CA, USA) following the protocol developed by Lan et al. [14] without any modification. The particle size and size distribution of microcapsule powders were measured using a Mastersizer 3000 equipped with Hydro LV (Malvern Instrument, Worcester, UK) by the method of Lan et al. without any changes [14]. Microstructure of eight microcapsule powders was imaged by scanning electron microscopy (SEM) (JEOL Model JSM-6490LV, MA, USA) and CLSM (Carl Zeiss Microscopy Ltd., Jena, Germany) as reported previously [14]. For the CLSM, an appropriate amount of dry powder was evenly distributed to fully cover the bottom of the μ-plate wells (μ-Plate 96 well, ibidi USA, Inc., Wisconsin), and then 200 μL of rhodamine B (0.5 mg/L) was added to the wells to stain protein. The samples were allowed to be incubated for 1h before observation. Images were taken at room temperature and acquired in 1024 × 1024 pixels using pre-installed image processing software.

2.7. Death rate of LGG in microcapsules powder during simulated sequential gastrointestinal (GI) digestion

To determine the viability of encapsulated LGG in the microcapsule powders over the period of simulated sequential GI digestion, 0.1 g of microcapsules was mixed with 9.9 mL of

simulated gastric fluid (SGF) (0.08 M HCl containing 0.2% w/w NaCl, pH 2.0) with 0.3% (w/v) pepsin in a tube and incubated in an orbital shaker (MaxQ™ 4000 Benchtop Orbital Shakers, Thermo Fisher Scientific Inc., USA) under 37 °C at 300 rpm for 2 h. The viable cells were measured at a 1h interval. After 2 h of incubation in SGF, the gastric digests were recovered by centrifugation at 8,000 rpm for 10 min, and then the collected powders (~ 0.1g) were added to 9.9 mL of simulated intestinal fluid (SIF) (0.05M KH_2PO_4, pH 7.4) containing 1.0% (w/v) bile salt and 1.0% (w/v) pancreatin [17, 18], followed by 2.5h incubation under 37 °C at 300 rpm. At each time point, the suspension of intestinal digests were taken to count the viable cells as reported previously [19]. Death rate of the encapsulated LGG at a given digestion time was calculated using Eq. (1).

$$\text{Death rate} = (1-\text{Log } N_t/ \text{ Log } N_0) \times 100\% \quad (1)$$

where N_t and N_0 were the viable cells at time t and time zero, respectively.

The viability and integrity of the encapsulated LGG during GI tract was also visualized using CLSM. The LIVE/DEAD BacLight bacterial viability kit (L-7012, Thermo fisher scientific, Inc. Waltham, MA, USA) with two color fluorochromes was applied to discriminate the alive cells from dead cells based on their cell membrane integrity [20]. In general, bacteria with intact cell membranes (alive) emit green fluorescence, whereas bacteria with damaged membranes (dead) emit red fluorescence [21]. According to the manufacture instruction, equal volumes of SYTO-9, a green-fluorescent nucleic acid dye (3.34 mM) and propidium iodide, a red-fluorescent nucleic acid dye (20 mM) in the kit were first mixed thoroughly, and then 3 μL of dye mixture was taken to dye 1.0 mL of the serial diluted digesta at each time point during digestion. For the microcapsule powder (before digestion), 10.0 mg microcapsules were first dissolved in 990.0 μL 10mM phosphate buffer (pH 7.0), and then 3.0 μL of dye mixture was

taken to dye 1.0 mL of the serial diluted samples. Subsequently, the mixture stayed in the dark for 15 min, and 200.0 μL of stained mixture was then placed on a μ-plate 96 well. Image was observed under CLSM at excitation/emission wavelength of 480 nm/500nm and 490 nm/635nm for SYTO-9 and propidium iodide, respectively.

2.8. Statistical analysis

The physicochemical properties of the complex coacervates were performed at least twice to confirm a consistent result. The viability of bacterial cells test and other measurements were repeated at least three times on freshly prepared samples and the values were expressed as means ± SD. Significant differences between means ($p < 0.05$) were statistically analyzed by one-way analysis of variance (ANOVA) (Version 9.3, SAS Institute Inc., NC, USA).

3.Results and discussions

3.1. Optimizing pH condition for complex coacervation formation

The formation of complex coacervates and the corresponding physiochemical properties highly rely on environmental pH, protein type, and protein–polysaccharide mixing ratio. Considering the application of complex coacervates in the field of encapsulation, a large number of researchers have suggested to fabricate microcapsules at the critical complex coacervation formation pH named pH_{opt}, under which the strongest electrostatic interaction is achieved between protein and polysaccharide. In this way, the maximum yield of complex coacervates is achieved [22]. As such, state diagram in conjunction with ζ-potential measurement were applied to elucidate the phase behavior of complex coacervates as a function of pH and to identify the pH_{opt} of complex coacervates [14]. According to our previous study, complex coacervation of PPI–SBP usually happened in the pH range of 5.0–2.5 [14]. Therefore, the phase behaviors of protein–SBP

mixtures with different mixing ratios as a function of pH (5.0–2.5) were evaluated after standing for 24h at 4 °C (**Fig. 1a**), and a state diagram was constructed as shown in **Fig. 1b**.

Fig. 1 inserted

At pH 5.0, clear phase separation occurred in the pure protein solutions (SC and PPI) at since it is close to their pIs, while precipitation and cloudy solution existed in all the tested samples except PPI: SBP ratio of 2:1 (P2) (**Fig. 1a**). This is mainly attributed to the electrostatic attraction between protein and SBP as suggested by the results of ζ-potential (**Fig. 1c**). For example, most of protein–SBP mixtures displayed intermediate ζ-potentials that were in between that of protein and SBP solutions. As the pH decreased from 5.0, more insoluble complexes were formed especially in the protein to SBP ratio of 5:1(e.g. C5 & P5), indicating the higher protein concentration combined with lower SBP concentration favorable insoluble complexes formation. This is because SBP is not sufficient enough to cover protein molecular at lower SBP concentration, thus protein aggregation plays the dominate role at pH 5. In our case, three distinguishable phase behaviors/appearances (turbid, precipitation and clear solution, precipitation and cloudy solution) were constructed and presented in the state diagram (**Fig. 1b**). According to the widely accepted definition of complex coacervates [14, 23], both precipitation and cloudy solution (▲) and precipitation and clear solution (■) of the biopolymer mixture presented in this study could be considered as complex coacervates bearing distinct structural and functional properties. In terms of application of complex coacervates in microencapsulation, the higher solid mass content of complex coacervates usually is associated with a greater encapsulation yield because of wall (e.g., coacervates) to core (e.g., bioactive compounds) ratio effect. In this study, precipitation and clear solution (■) displayed a higher amount of solid mass than precipitation and cloud solution (▲). This is because stronger electrostatic interactions

between protein and SBP were exhibited in precipitation and clear solution (■) phase separation, leading to a larger coacervates yield. Consequently, precipitation & clear solution (■) phase behavior is more suitable to encapsulate probiotics than precipitation & cloud solution (▲) phase in our study. Such conclusion was further confirmed by the ζ-potential results (**Fig. 1c**). In general, the precipitation phenomenon between protein and polysaccharide tends to be more obvious under an environment where a greater strength of electrostatic attraction is provided. Concomitantly, the net surface charge of the mixture is close to zero. As marked in **Fig. 1c**, the three dash lines indicated the zero net charge of the two proteins (SC and PPI)–SBP mixtures with two different mixing ratios at various pH ranging from ~3.7 to 2.5. It is noted that all of the four treatments produced precipitation & clear solution (■) phase at pH between 3.0 –2.5 (**Fig. 1b**).

Regarding the impact of protein–SBP mixing ratio on phase behavior of the mixture, the occurrence of precipitation and clear solution (■) was shifted towards more acidic pH as the protein–SBP ratio decreased. This phenomenon was also in agreement with other studies [24, 25]. It suggested that phase behavior of complex coacervates can be influenced by altering the charge of one or both biopolymer macroions through changing environmental pH, and/or the mixing ratios of the biopolymers. Combing state diagram and ζ-potential results, as well as the potential impact of pH on the viability of probiotics, pH 3.0 was selected as the optimum pH for preparing protein–SBP complex coacervates in the following experiments.

3.2. Viscoelastic and microstructure properties of wet microcapsules

3.2.1. Viscoelastic properties

Viscoelastic properties of complex coacervates not only provide insight on intermolecular interactions of biopolymers, but also furnish a useful information about the textual properties of

final food products [26]. Herein, the storage modulus (G') and loss modulus (G") of the wet complex coacervates containing probiotics prepared at pH 3.0 over the angular frequency range of 0.01–100 rad/s were determined, and the results were shown in **Fig. 2a**.

Fig. 2 inserted

In this study, the G' of all the samples was higher than G", which usually reflected a gel-like network structure [26-28]. This result suggested that the network structure between protein (SC or PPI) and SBP was successfully formed at pH 3.0 in all tested samples. From **Fig. 2a**, the highest to lowest G' in the tested samples were C5, C2, P5, and P2. Since a higher G' typically indicates a stronger interaction between the biopolymers, the results suggest that the overall interaction strength of SC–SBP samples was stronger than that of PPI–SBP samples. This different interaction strength between the two proteins with the same SBP might have attributed to the varied protein gel and complex coacervates structure between SC–SBP and PPI–SBP at acidic pH. In general, acidic pH promotes the formation of protein gel. By adding polysaccharide in acidic protein solution, both protein gelling and complex coacervation of protein and polysaccharide could happen simultaneously. Previous study proposed that SBP generally adsorbed on the surface of SC micelle aggregates to form SC–SBP complexes at acidic pH [29]. By contrast, positive patch of PPI molecules could adsorb on the segments of an anionic SBP molecule and form an intramolecular complex coacervates. Additionally, SC gel had a higher gel strength compared to PPI gel at the same protein concentration. This is because particulate gel of PPI through protein aggregation had limited amount of junction zones compared to SC ones. As a result, the distinguishable viscoelastic properties of complex coacervates from two different proteins were observed. In terms of protein to SBP ratio, both dynamic moduli (G' and G") of the complex coacervates were decreased upon the increase of SBP percentage, which was in line

with our previous study [14]. This could be explained by the interference of polysaccharide for the aggregation of protein gel structure which prevented the formation of protein strands and clusters [30]. Consequently, both dynamic moduli (G' and G'') were decreased with increasing SBP concentration.

3.2.2. Microstructure

In order to better understand the impact of protein type and protein to polysaccharide mixing ratio on physical properties of the complex coacervates, the microstructure of the same sample set (wet complex coacervates) used in rheological experiment were characterized via CLSM (**Fig. 2b)**. In general, the microstructure of the complex coacervates was greatly impacted by protein type in the biopolymer mixtures since protein accounted for the majority of the ingredients in the protein–SBP–probiotics ternary system. For example, at a relative low SBP content in the ternary mixture (protein to SBP ratio of 5:1, **Fig. 2b i**), the microstructure of SC–SBP was more like acid casein gel, featuring two distinct structures; these were the coherent network with large pores composed of casein micelles, and strands and clusters combined with SBP that absorbed on the surface of casein micelles. As the SBP concentration increased in this system, the microstructure was altered dramatically as reflected by the presence of a large amount of small pores in the gel network, which was in line with previous study [30-32]. On the other hand, highly cross-linked gel network with condensed globule aggregation were observed in PPI–SBP system (**Fig. 2b iii**). Interestingly, altering the concentration of SBP did not impose drastic impact on the microstructure of PPI–SBP complex coacervates in this study (**Fig. 2b iv**).

3.3. Impact of drying methods on physical properties of dried microcapsules

3.3.1 FTIR

FTIR was employed to further understand the interaction of the functional groups between the protein (SC or PPI) and SBP, as well as the impact of drying methods on such interaction.

Fig. 3 inserted

The spectra of the control samples (SC, PPI, and SBP) were consistent with previous reports [14, 33, 34]. Different drying methods did not exert any appreciable impact on the interactions among functional groups as indicated by these identical spectra. In terms of the dried complex coacervates, their spectra in the higher wavenumber region (1450–4000 cm^{-1}) were mainly dominated by the proteins, and the higher the protein ratio, the more similarities they displayed (**Fig. 3a&b**). On the other hand, pectin dominated the spectra in the lower wavenumber part (700–1450 cm^{-1}) which was corroborated by the serried peaks, such as the peaks at 1016 and 1047 cm^{-1}, associated with the functional groups of pectin [35, 36]. In addition, the distinct peak at 1731 cm^{-1} in SBP became a shoulder-like region in all tested complex coacervates around the same wavenumber, and the symmetric $-COO^-$ stretching vibration (1620 cm^{-1}) in SBP shifted slightly toward the amide I group (1633 cm^{-1}) when forming the complex coacervates (as pointed by the dash line in **Fig. 3**). Besides, peaks at 1438 cm^{-1} and 1369 cm^{-1} found in SBP, as well as the amide III group region from the protein were significant influenced by the protein−SBP complex coacervation. For example, some characteristic peaks in the initial biopolymers such as 1620 cm^{-1} of SBP, 1392 cm^{-1} of SC, and 1394 cm^{-1} of PPI, were vanished in all protein−SBP complex coacervates indicating electrostatic interaction occurred between the amine groups of protein ($-NH_4^+$) and carboxyl groups of SBP ($-COO^-$). Similar results were

also reported in various complex coacervation systems, e.g. the fish skin gelatin and gum Arabic complex coacervation [37] and the interaction between egg white protein and xanthan gum [38], where electrostatic interaction was proved to be the major driven force for the formation of complex coacervations.

3.3.2. Particle size

The results of particle size distribution of the dried microcapsules as influenced by protein type and drying methods were shown in **Fig. 4**, and the particle size $D_{(50)}$ of the samples were also measured as supportive data as shown in Table S-1. We observed the higher SBP content led to the formation of bigger particles in spray-dried samples. This could be explained by the intensive involvement of SBP chains in the complex coacervates, particularly in the higher SBP ratio, thus promoting the formation of a bigger structure. More specifically, we noticed that the SC−SBP microcapsules (both spray-dried and freeze-dried) showed a monomodal particle size distribution. As to the PPI−SBP microcapsules, they all presented multimodal particle size distributions among the range of 0.05−1,000 μm. The spray dried PPI−SBP microcapsules had wider size ranges than the freeze-dried counterparts. For example, the P2-S displayed three peaks with huge size differences, as smallest as ~0.4 μm and largest as ~600 μm, which was also confirmed by SEM (**Fig. 5**). The presence of non-uniform particle size of spray-dried PPI was also reported in our previous study [33], which might be generated by the different fractions (e.g., albumin, vicilin, and legumin) of PPI interacting with SBP to form particles with variable size [39]. Conversely, the freeze-dried PPI−SBP microcapsules (**Fig. 4**) were mostly distributed in a bigger but narrower size range (80−100 μm). It was worth noting that the longer freeze-drying time (> 48 h) may promote the aggregation of complex coacervates to form

big chunk of flakes, which would remain intact with a mild manual milling process after freeze-drying.

Fig. 4 inserted

3.3.3. Microstructure

The microstructures of the dried microcapsules were investigated by CLSM and SEM. Since the drying processing played a crucial role on the microstructure and the location/distribution of LGG, we displayed all the images by grouping them in light of drying processing rather than the protein type. Firstly, CLSM was applied to visualize the microstructures of the spray-dried and freeze-dried microcapsules by staining protein with rhodamine B (first row in **Fig. 5a&b**). Compared with the images in **Fig. 2b** which displayed the microstructure of the wet complex coacervates, it was clear that drying methods remarkably changed the morphology of the dried microcapsules in multiple ways. For example, all the spray-dried microcapsules exhibited a spherical shape due to the nature of spray-drying process. By contrast, freeze-drying process converted the liquid complex coacervates to a lamellar, scale-like structure, and no significant structural difference was found between samples. Such observation was reasonable since i) both the pre-freeze treatment (frozen in -80 ℃ freezer for 2h) prior to freeze-drying and the freeze-drying process itself promoted the conjugation of the complex coacervates particles into bigger and flat pieces; ii) the samples were ground to a maximum extent with manual mortar and pestle grinding. Similar phenomenon was also reported in gelatin− gum Arabic and chitosan−carboxymethylcellulose systems [40]. In terms of protein type, all dried microcapsules with PPI showed smaller spherical particles, but contained more un-uniform particle aggregates compared to SC microcapsules, which was in line with the particle size results (**Fig. 4**).

Fig. 5 inserted

The microstructure of the dried microcapsules and the distribution of LGG probiotics within the matrix (pointed by the arrows) were further investigated by SEM under different magnifications (below the corresponding CLSM images in **Fig. 5**). In general, the spray-dried samples presented mostly spherical shape with cavities and creases caused by the rapid loss of moisture during spray-drying [41, 42], with varied particle sizes among samples. Moreover, the outer topography of the particles indicated that the shell was intact, with the absence of rupture and visible broken shells. In addition to the insights gained in the microstructure of the dried microcapsules, we also acquired that the bacterial cells LGG were successfully encapsulated, but randomly distributed within biopolymer matrixes (as indicated by the arrows in **Fig. 5a**). Regarding the protein type in the spray-dried microcapsules, the SC−SBP samples seemed to have a greater shrinkage due to the presence of some severely contracted particles and more crumpled surface (as circled in **Fig. 5a**). Previous study also indicated that the presence of different biopolymers as wall matrices led to varied microstructure of spherical particles during spray-drying [43].

For the freeze-dried samples, tiny pieces of the samples without grinding were applied to SEM directly to maintain the original microstructure of the microcapsules (below the corresponding CLSM images **Fig. 5b**). As illustrated from the images under×100 magnification, the overall structure of the samples was highly bonded with porous sponge network, similar to the previously reported results [44], and a clear structure can be visualized in the image with a magnification of ×1,000. Regardless of protein type, samples with a higher protein ratio (5:1) always exhibited a denser and more compact structure compared to a lower protein ratio (2:1) ones, especially in PPI group. When protein type was taken into consideration, the network in

PPI−SBP samples was apparently thinner and more fragile with larger pore sizes when compared to that in SC−SBP samples, which meant the P2-F sample possessed a distinguish poor structure among the freeze-dried samples. This conclusion was further confirmed by the images under ×7,500 magnification where it appears that some of the structures were supported by the bacteria (P2-F). One potential reason might be due to the lower viscoelastic properties of the wall materials (**Fig. 2a)**.

Fig. 5 inserted

3.4. The death rate of encapsulated LGG in microcapsules during simulated sequential gastrointestinal digestion

The death rate of LGG in each dried microcapsule at chosen time point during simulated gastrointestinal sequential digestion was compared (**Fig. 6)**. The viable cell count of each sample was at 8.5−9 Log CFU/g before digestion and had no significant difference ($p < 0.05$) among the samples (**Table S-2**).

Fig. 6 inserted

As shown in **Fig. 6a**, in the period of simulated gastric digestion (SGD), the death rate of all spray-dried samples remained at a very low level (< 10%) with no significant difference (p <0.05). This was reasonable since the structure of spray-dried microcapsules maintained very well at acidic pH. Interestingly, it could be noticed that LGG in the microcapsules with a higher protein content presented a greater death rate during SGD (e.g., C5-S *vs* C2-S). Part of the reason might be derived from their particle size differences. In general, C5-S samples had a relatively smaller particle size compared to C2-S (**Fig. 4**). As such, they would have a relatively larger surface area for pepsin and H^+ to access, thus leading to the death of LGG. After transferred to

the simulated intestinal digestion (SID) for 1h, we noticed a drastic increase of death rate of all the samples, especially when SC was presented. This was because the gradual disassociation of the complex coacervates structure under the SID condition, and the collapse of the gel-like structure allowed the hydrolytic enzymes and salts to be more accessible to the bacteria. The reason that SC group showed worse protective effect in SID rather than PPI group could be mainly due to their different microstructures. Spray-dried microcapsules with PPI as protein source showed a wider range of particle size distribution in conjunction with smooth surface compared with those containing SC. Previous study concluded that the particle size and smoothness of the microcapsules greatly influenced the viability of the encapsulated cells. The better protection for encapsulated cells was postulated to be largely originated from the relatively smooth surface of microcapsules that had higher integrity of particles and lower permeability of oxygen and simulated GI fluid [45]. In the last 1.5 h of SID, a slight increase in the death rate was observed in spray-dried PPI−SBP microcapsules, in which more than 7.5 Log CFU/g viable cells were maintained (**Table S-2**). As for the spray-dried SC−SBP samples, they were still able to maintain a population of probiotics higher than 6 Log CFU/g, albeit they provided a relatively less protection to the cells. The protein to polysaccharide ratio did not show obvious influence on the death rate of LGG in spray-dried samples; however, widening the current ratios in further study is possibly necessary to confirm this conclusion.

By contract to the spray-dried sample, a consistent tendency was found in the freeze-dried microcapsules over the entire course of the simulated digestion (**Fig. 6b**). The death rate rose gradually with increasing digestion time. Overall, the performance of the spray-dried samples was superior to those of the freeze-died counterparts in terms of death rate during GI tract, which indicated that the morphological properties of microcapsules affected the rate of the

hydrolysis reaction to a greater extent. Zhao et al. [12] also reported that spray-drying possess improved mechanical strength and barrier property of the complex coacervates. As denoted by the SEM result, spray-dried samples had more intact and integrated structures than freeze-dried samples. In terms of protein sources, the freeze-dried PPI−SBP samples had a poor ability to protect the bacteria when exposed to digestive environment at the beginning, but the death rate of freeze-dried SC−SBP microcapsules during gastric digestion was comparable to that of the spray-dried SC−SBP samples. This also could be explained by the microstructural differences revealed by the SEM images in **Fig. 5**, where the P5-F and P2-F samples exhibited more porous and thinner structure compared to C5-F and C2-F, especially for P2-F. When all the microcapsules reached the end of the simulated digestion time, C2-F had the greatest protective effect on the viability of LGG among all the freeze-dried samples.

In addition, the changes of live cells during simulated gastrointestinal sequential digestion were investigated using CLSM images (**Fig. 6c**). Herein, we only demonstrated the images of each protein with one protein−polysaccharide ratio (2:1) because their much similarities with altered ratio. As one can see, there were numerous live cells (green ones) visible in all dried microcapsules before digestion. After the gastric digestion, only a few cells remained alive while most of them dead (red ones). After further digested in the intestinal condition, the viable cells were fewer as we expected. Although these images were not proportionally correlated to the death rate of each sample shown in **Fig. 6a&b**, this was reasonable because only a tiny proportion of the sample could be presented in the images under CLSM observation and usually the death of cells was found exponentially. Interestingly, more live cells appeared in all freeze-dried samples (C2-F and P2-F) rather than in spray-dried samples before digestion. One reason might be attributed to the different solubility of microcapsules powder. To stain the

cells in the microcapsules for CLSM, the sample powder has to be dissolved in the buffer system. We noticed that the freeze-dried samples had a higher dissolution rate and solubility compared to the spray-dried ones. This might be part of factors contributing to a higher death rate of probiotics in the freeze-dried microcapsules compared to spray-dried ones during digestion.

4. Conclusions

In this work, the effects of pH (2.5–5.0), protein type (SC or PPI), and protein to SBP mixing ratio (5:1 or 2:1) on the formation and microstructure of complex coacervates were systematically investigated. The ζ-potential and FTIR results indicated that complex coacervates were successfully formed primarily through electrostatic interaction in all tested systems at pH 3.0. The formation of a gel-like structure was confirmed by their viscoelastic properties. Both SC−SBP and PPI−SBP complex coacervates formed at pH 3.0 were applied to encapsulate LGG probiotics, and two different drying methods (spray-drying and freeze-drying) were applied to convert liquid complex coacervates into convenient powder form. The particle size, morphological properties of microcapsules, and their protective effect on the viability of encapsulated LGG during simulated sequential GI digestion were assessed. The results indicated that spray-dried microcapsules presented a uniform spherical shape and smooth surface, while the freeze-dried ones were shattered, scale-like and porous, which mainly resulted in overall better protection of spray-dried samples on LGG than that of freeze-dried samples. Considering the impact of protein type, PPI−SBP microcapsules generally had a widely distributed multimodal particle size, whereas the SC−SBP microcapsules had monomodal distributed particle size. Moreover, recognizable differences on the microstructure of microcapsules formed by difference protein from the same drying processing could be observed. Spray-dried SC−SBP

microcapsules possessed severely shrunken and crumped surface compared to spray-dried PPI−SBP ones. Consequently, LGG in spray-dried PPI−SBP microcapsules had a lower death rate than that in SC−SBP over the course of simulated sequential GI digestion. Therefore, among all the samples, P2-S (spray-dried LGG microcapsules at the PPI−SBP ratio of 2:1) and P5-S (spray-dried LGG microcapsules at the PPI−SBP ratio of 5:1) showed the supreme protection to the encapsulated LGG, followed by C5-S (spray-dried LGG microcapsules at the SC−SBP ratio of 5:1), and maintained a number of over 7 Log CFU/g viable cells after digestion. Overall, the selection of protein type as well as the designing of a proper drying processing are necessary to ensure the viability of the encapsulated probiotics by means of complex coacervation. More importantly, the results revealed the great potential of plant-based protein being used as deliver material of probiotics by complex coacervation and applied in food industry.

Acknowledgement

This work is supported by USDA National Institute of Food and Agriculture (Hatch ND1594). A scholarship for Ms. Xiaoxi Qi is provided by the China Scholarship Council (CSC).

References

1. M. Sanders, D. Merenstein, C. Merrifield and R. Hutkins, Probiotics for human use, *Nutrition bulletin*, 2018, **43**, 212-225.
2. Y. Doleyres and C. Lacroix, Technologies with free and immobilised cells for probiotic bifidobacteria production and protection, *International Dairy Journal*, 2005, **15**, 973-988.
3. H. Liu, J. Gong, D. Chabot, S. S. Miller, S. W. Cui, F. Zhong and Q. Wang, Improved survival of Lactobacillus zeae LB1 in a spray dried alginate-protein matrix, *Food Hydrocolloids*, 2018, **78**, 100-108.
4. Y. P. Timilsena, B. Wang, R. Adhikari and B. Adhikari, Advances in microencapsulation of polyunsaturated fatty acids (PUFAs)-rich plant oils using complex coacervation: A review, *Food Hydrocolloids*, 2017, **69**, 369-381.
5. E. Adal, A. Sadeghpour, S. Connell, M. Rappolt, E. Ibanoglu and A. Sarkar, Heteroprotein complex formation of bovine lactoferrin and pea protein isolate: A multiscale structural analysis, *Biomacromolecules*, 2017, **18**, 625-635.
6. M. C. E. Ribeiro, K. S. Chaves, C. Gebara, F. N. S. Infante, C. R. F. Grosso and M. L. Gigante, Effect of microencapsulation of Lactobacillus acidophilus LA-5 on

physicochemical, sensory and microbiological characteristics of stirred probiotic yoghurt, *Food Research International*, 2014, **66**, 424-431.
7. C. L. Gerez, G. Font de Valdez, M. L. Gigante and C. R. F. Grosso, Whey protein coating bead improves the survival of the probiotic Lactobacillus rhamnosus CRL 1505 to low pH, *Letters in Applied Microbiology*, 2012, **54**, 552-556.
8. L. Bosnea, T. Moschakis and C. Biliaderis, Microencapsulated cells of Lactobacillus paracasei subsp. paracasei in biopolymer complex coacervates and their function in a yogurt matrix, *Food Function*, 2017, **8**, 554-562.
9. Y. Lan, B. Chen and J. Rao, Pea protein isolate–high methoxyl pectin soluble complexes for improving pea protein functionality: Effect of pH, biopolymer ratio and concentrations, *Food Hydrocolloids*, 2018, **80**, 245-253.
10. D. Eratte, K. Dowling, C. J. Barrow and B. Adhikari, Recent advances in the microencapsulation of omega-3 oil and probiotic bacteria through complex coacervation: A review, *Trends in Food Science & Technology*, 2018, **71**, 121-131.
11. M. Zhao, Y. Wang, X. Huang, M. Gaenzle, Z. Wu, K. Nishinari, N. Yang and Y. Fang, Ambient storage of microencapsulated Lactobacillus plantarum ST-III by complex coacervation of type-A gelatin and gum arabic, *Food Function*, 2018, **9**, 1000-1008.
12. M. Zhao, X. Huang, H. Zhang, Y. Zhang, M. Gänzle, N. Yang, K. Nishinari and Y. Fang, Probiotic encapsulation in water-in-water emulsion via heteroprotein complex coacervation of type-A gelatin/sodium caseinate, *Food Hydrocolloids*, 2020, **105**, 105790.
13. S. Liu, C. Elmer, N. H. Low and M. T. Nickerson, Effect of pH on the functional behaviour of pea protein isolate–gum Arabic complexes, *Food Research International*, 2010, **43**, 489-495.
14. Y. Lan, J.-B. Ohm, B. Chen and J. Rao, Phase behavior and complex coacervation of concentrated pea protein isolate-beet pectin solution, *Food Chemistry*, 2020, **307**, 125536.
15. S. Huang, M.-L. Vignolles, X. D. Chen, Y. Le Loir, G. Jan, P. Schuck and R. Jeantet, Spray drying of probiotics and other food-grade bacteria: A review, *Trends in Food Science & Technology*, 2017, **63**, 1-17.
16. C. Iaconelli, G. Lemetais, N. Kechaou, F. Chain, L. G. Bermúdez-Humarán, P. Langella, P. Gervais and L. Beney, Drying process strongly affects probiotics viability and functionalities, *Journal of Biotechnology*, 2015, **214**, 17-26.
17. A. V. Rao, N. Shiwnarain and I. Maharaj, Survival of Microencapsulated Bifidobacterium pseudolongum in Simulated Gastric and Intestinal Juices, *Canadian Institute of Food Science and Technology Journal*, 1989, **22**, 345-349.
18. M. Xu, F. Gagné-Bourque, M.-J. Dumont and S. Jabaji, Encapsulation of Lactobacillus casei ATCC 393 cells and evaluation of their survival after freeze-drying, storage and under gastrointestinal conditions, *Journal of Food Engineering*, 2016, **168**, 52-59.
19. X. Qi, S. Simsek, J.-B. Ohm, B. Chen and J. Rao, Viability of Lactobacillus rhamnosus GG microencapsulated in alginate/chitosan hydrogel particles during storage and simulated gastrointestinal digestion: role of chitosan molecular weight, *Soft Matter*, 2020, **16**, 1877-1887.
20. J. Guerin, J. Burgain, F. Borges, B. Bhandari, S. Desobry, J. Scher and J. Scher, Use of imaging techniques to identify efficient controlled release systems of Lactobacillus rhamnosus GG during in vitro digestion, *Food Function*, 2017, **8**, 1587-1598.

21. A. Atia, A. Gomaa, I. Fliss, E. Beyssac, G. Garrait and M. Subirade, A prebiotic matrix for encapsulation of probiotics: physicochemical and microbiological study, *Journal of Microencapsulation*, 2016, **33**, 89-101.
22. A. K. Stone, A. Teymurova, C. Chang, L. Cheung and M. T. Nickerson, Formation and functionality of canola protein isolate with both high- and low-methoxyl pectin under associative conditions, *Food Science and Biotechnology*, 2015, **24**, 1209-1218.
23. T. Moschakis and C. G. Biliaderis, Biopolymer-based coacervates: Structures, functionality and applications in food products, *Current Opinion in Colloid & Interface Science*, 2017, **28**, 96-109.
24. P. K. S. Pillai, A. K. Stone, Q. Guo, Q. Guo, Q. Wang and M. T. Nickerson, Effect of alkaline de-esterified pectin on the complex coacervation with pea protein isolate under different mixing conditions, *Food Chemistry*, 2019, **284**, 227-235.
25. D. Thakur, A. Jain, G. Ghoshal, U. S. Shivhare and O. P. Katare, Microencapsulation of β-carotene based on casein/guar gum blend using zeta potential-yield stress phenomenon: an approach to enhance photo-stability and retention of functionality, *AAPS PharmSciTech*, 2017, **18**, 1447-1459.
26. J. Liu, Y. Y. Shim, J. Shen, Y. Wang and M. J. T. Reaney, Whey protein isolate and flaxseed (Linum usitatissimum L.) gum electrostatic coacervates: Turbidity and rheology, *Food Hydrocolloids*, 2017, **64**, 18-27.
27. M. Raei, A. Rafe and F. Shahidi, Rheological and structural characteristics of whey protein-pectin complex coacervates, *Journal of Food Engineering*, 2018, **228**, 25-31.
28. H. Espinosa-Andrews, O. Sandoval-Castilla, H. Vázquez-Torres, E. J. Vernon-Carter and C. Lobato-Calleros, Determination of the gum Arabic–chitosan interactions by Fourier Transform Infrared Spectroscopy and characterization of the microstructure and rheological features of their coacervates, *Carbohydrate Polymers*, 2010, **79**, 541-546.
29. X. Li, Y. Fang, G. O. Phillips and S. Al-Assaf, Improved sugar beet pectin-stabilized emulsions through complexation with sodium caseinate, *Journal of Agricultural and Food Chemistry*, 2013, **61**, 1388-1396.
30. L. Matia-Merino, K. Lau and E. Dickinson, Effects of low-methoxyl amidated pectin and ionic calcium on rheology and microstructure of acid-induced sodium caseinate gels, *Food Hydrocolloids*, 2004, **18**, 271-281.
31. J. A. Lucey, M. Tamehana, H. Singh and P. A. Munro, A comparison of the formation, rheological properties and microstructure of acid skim milk gels made with a bacterial culture or glucono-δ-lactone, *Food Research International*, 1998, **31**, 147-155.
32. B. Sołowiej, P. Glibowski, S. Muszyński, J. Wydrych, A. Gawron and T. Jeliński, The effect of fat replacement by inulin on the physicochemical properties and microstructure of acid casein processed cheese analogues with added whey protein polymers, *Food Hydrocolloids*, 2015, **44**, 1-11.
33. Y. Lan, M. Xu, J.-B. Ohm, B. Chen and J. Rao, Solid dispersion-based spray-drying improves solubility and mitigates beany flavour of pea protein isolate, *Food Chemistry*, 2019, **278**, 665-673.
34. D. M. Curley, T. F. Kumosinski, J. J. Unruh and H. M. Farrell, Changes in the secondary structure of bovine casein by fourier transform infrared spectroscopy: Effects of calcium and temperature, *Journal of Dairy Science*, 1998, **81**, 3154-3162.
35. A. Synytsya, J. Čopíková, P. Matějka and V. Machovič, Fourier transform Raman and infrared spectroscopy of pectins, *Carbohydrate Polymers*, 2003, **54**, 97-106.

36. S. Posé, A. R. Kirby, J. A. Mercado, V. J. Morris and M. A. Quesada, Structural characterization of cell wall pectin fractions in ripe strawberry fruits using AFM, *Carbohydrate Polymers*, 2012, **88**, 882-890.
37. Y. Li, X. Zhang, Y. Zhao, J. Ding and S. Lin, Investigation on complex coacervation between fish skin gelatin from cold-water fish and gum arabic: Phase behavior, thermodynamic, and structural properties, *Food Research International*, 2018, **107**, 596-604.
38. C. J. F. Souza and E. E. Garcia-Rojas, Interpolymeric complexing between egg white proteins and xanthan gum: Effect of salt and protein/polysaccharide ratio, *Food Hydrocolloids*, 2017, **66**, 268-275.
39. Y. Yuan, Z.-L. Wan, X.-Q. Yang and S.-W. Yin, Associative interactions between chitosan and soy protein fractions: Effects of pH, mixing ratio, heat treatment and ionic strength, *Food Research International*, 2014, **55**, 207-214.
40. N. Kanha, J. M. Regenstein, S. Surawang, P. Pitchakarn and T. Laokuldilok, Properties and kinetics of the in vitro release of anthocyanin-rich microcapsules produced through spray and freeze-drying complex coacervated double emulsions, *Food Chemistry*, 2021, **340**, 127950.
41. A. M. M. Costa, J. C. Nunes, B. N. B. Lima, C. Pedrosa, V. Calado, A. G. Torres and A. P. T. R. Pierucci, Effective stabilization of CLA by microencapsulation in pea protein, *Food Chemistry*, 2015, **168**, 157-166.
42. S. F. Subtil, G. A. Rocha-Selmi, M. Thomazini, M. A. Trindade, F. M. Netto and C. S. Favaro-Trindade, Effect of spray drying on the sensory and physical properties of hydrolysed casein using gum arabic as the carrier, *Journal of Food Science and Technology*, 2014, **51**, 2014-2021.
43. T. Tao, Z. Ding, D. Hou, S. Prakash, Y. Zhao, Z. Fan, D. Zhang, Z. Wang, M. Liu and J. Han, Influence of polysaccharide as co-encapsulant on powder characteristics, survival and viability of microencapsulated Lactobacillus paracasei Lpc-37 by spray drying, *Journal of Food Engineering*, 2019, **252**, 10-17.
44. R. Rajam and C. Anandharamakrishnan, Spray freeze drying method for microencapsulation of Lactobacillus plantarum, *Journal of Food Engineering*, 2015, **166**, 95-103.
45. D. Kalita, S. Saikia, G. Gautam, R. Mukhopadhyay and C. L. Mahanta, Characteristics of synbiotic spray dried powder of litchi juice with Lactobacillus plantarum and different carrier materials, *LWT*, 2018, **87**, 351-360.

Figure

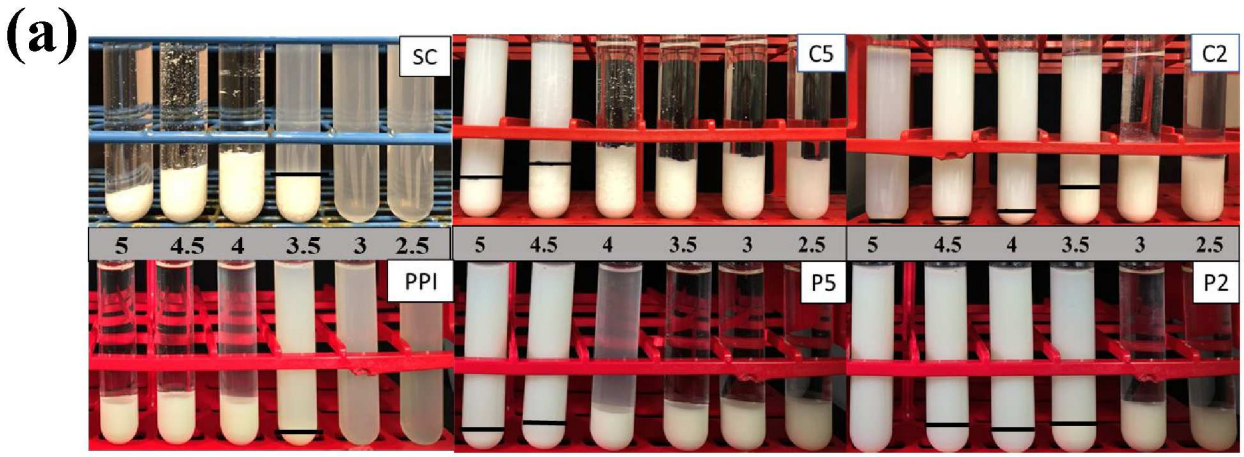
(a)
SC
C5
C2
5 4.5 4 3.5 3 2.5
5 4.5 4 3.5 3 2.5
5 4.5 4 3.5 3 2.5
PPI
P5
P2

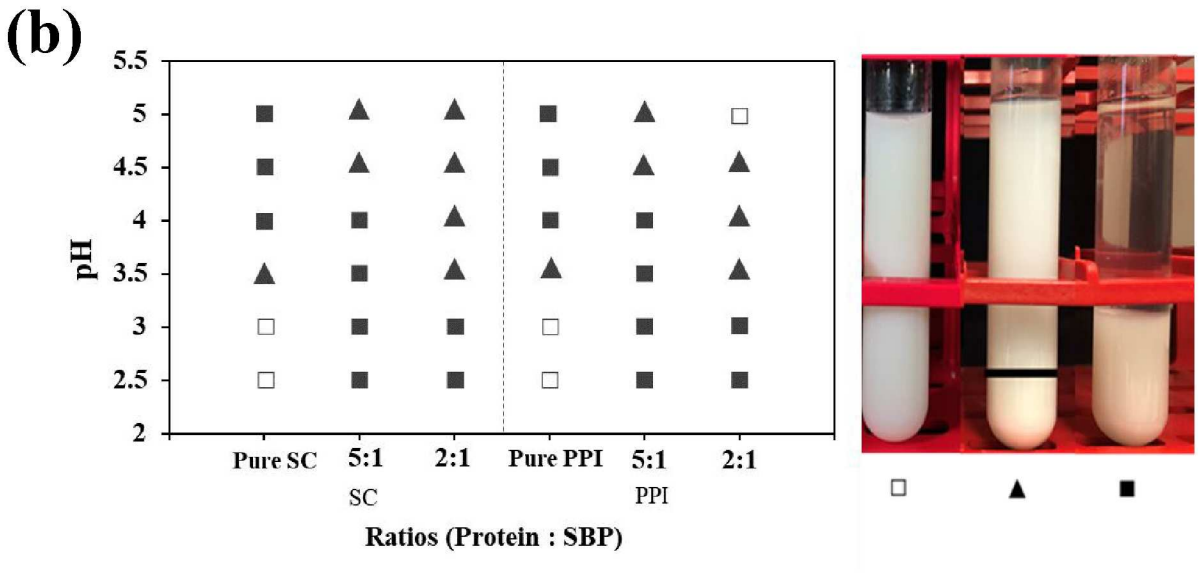
(b)
5.5
5
4.5
4
3.5
3
2.5
2
pH
Pure SC
5:1
2:1
Pure PPI
5:1
2:1
SC
PPI
Ratios (Protein : SBP)

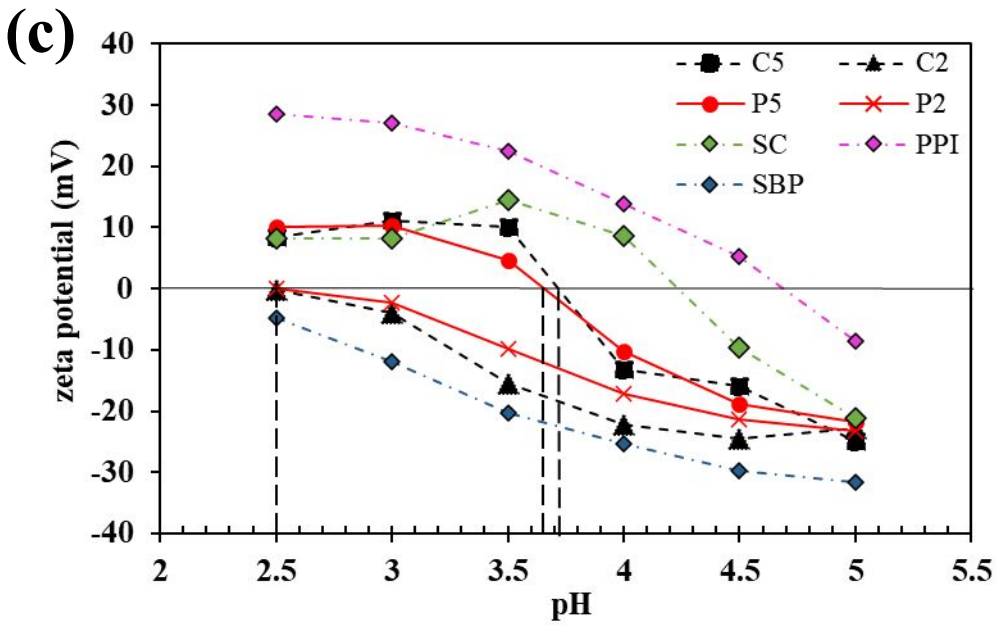

Fig. 1. (a) The appearance of SC, PPI, SC-SBP and PPI-SBP mixture at different mixing ratios as function of pH. The appearance was observed after 24 h standing. (b) State diagram of SC, PPI, SC-SBP and PPI-SBP mixtures at different mixing ratios during acid titration□ represents turbid solution; ▲ represents precipitation and cloudy solution; ■ represents precipitation and clear solution. (c) The dependence of zeta potential of SC, PPI, SBP, SC-SBP and PPI-SBP mixtures at different mixing ratios on pH values.

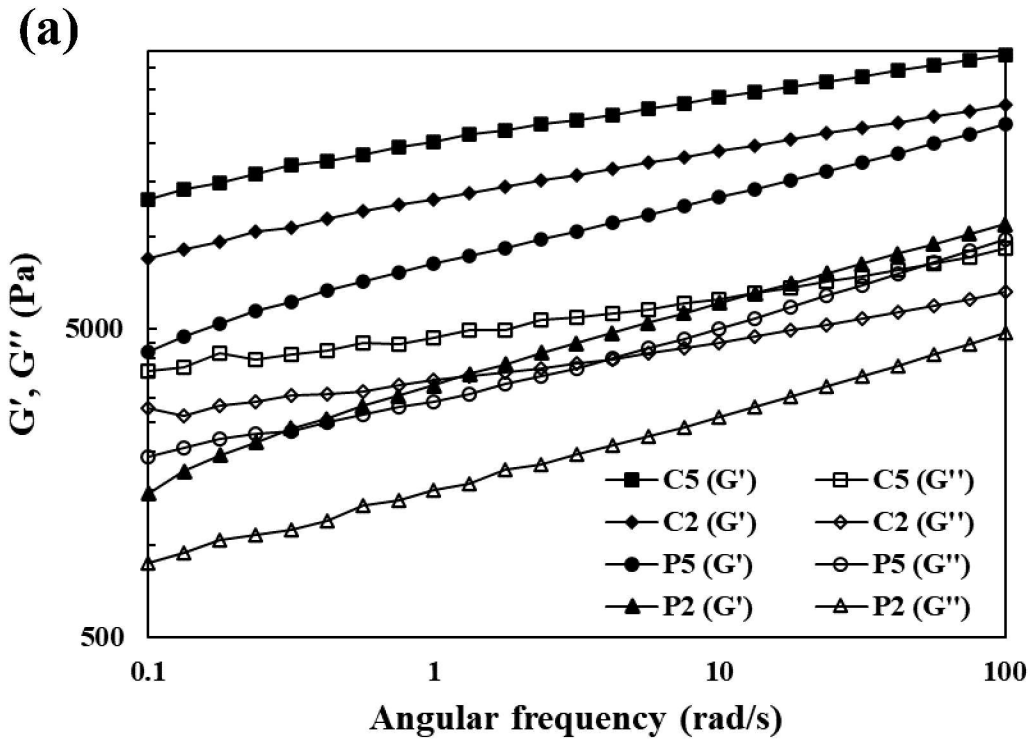
(a)
G', G'' (Pa)
5000
500
0.1
1
10
100
Angular frequency (rad/s)
C5 (G')
C5 (G'')
C2 (G')
C2 (G'')
P5 (G')
P5 (G'')
P2 (G')
P2 (G'')

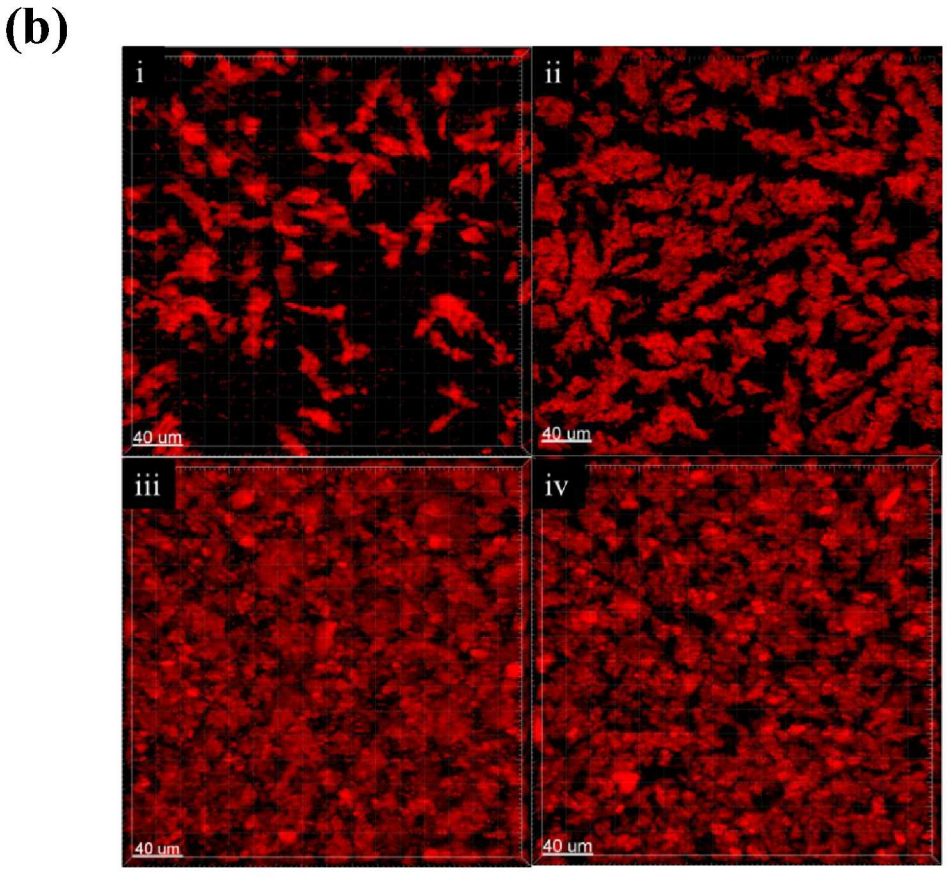
(b)
i
ii
iii
iv
40 um
40 um
40 um
40 um

Fig. 2. (a) The impact of protein to SBP mixing ratios (5:1 and 2:1) on storage modulus G'; and loss modulus G" of the complex coacervates at 1 rad/s frequency under pH 3.0. (b) The confocal laser scanning microscopy (CLSM) images of liquid SC–SBP and PPI–SBP complex coacervates prepared at pH 3.0 and mixing ratio of 5:1 and 2:1. (i) C5; (ii) C2; (iii) P5; and (iv) P2. C5 represents SC–SBP complex coacervates prepared at 5:1 mixing ratio; C2 represents SC–SBP complex coacervates prepared at 2:1 mixing ratio; P5 represents PPI–SBP complex coacervates prepared at 5:1 mixing ratio; P2 represents PPI–SBP complex coacervates prepared at 2:1 mixing ratio.

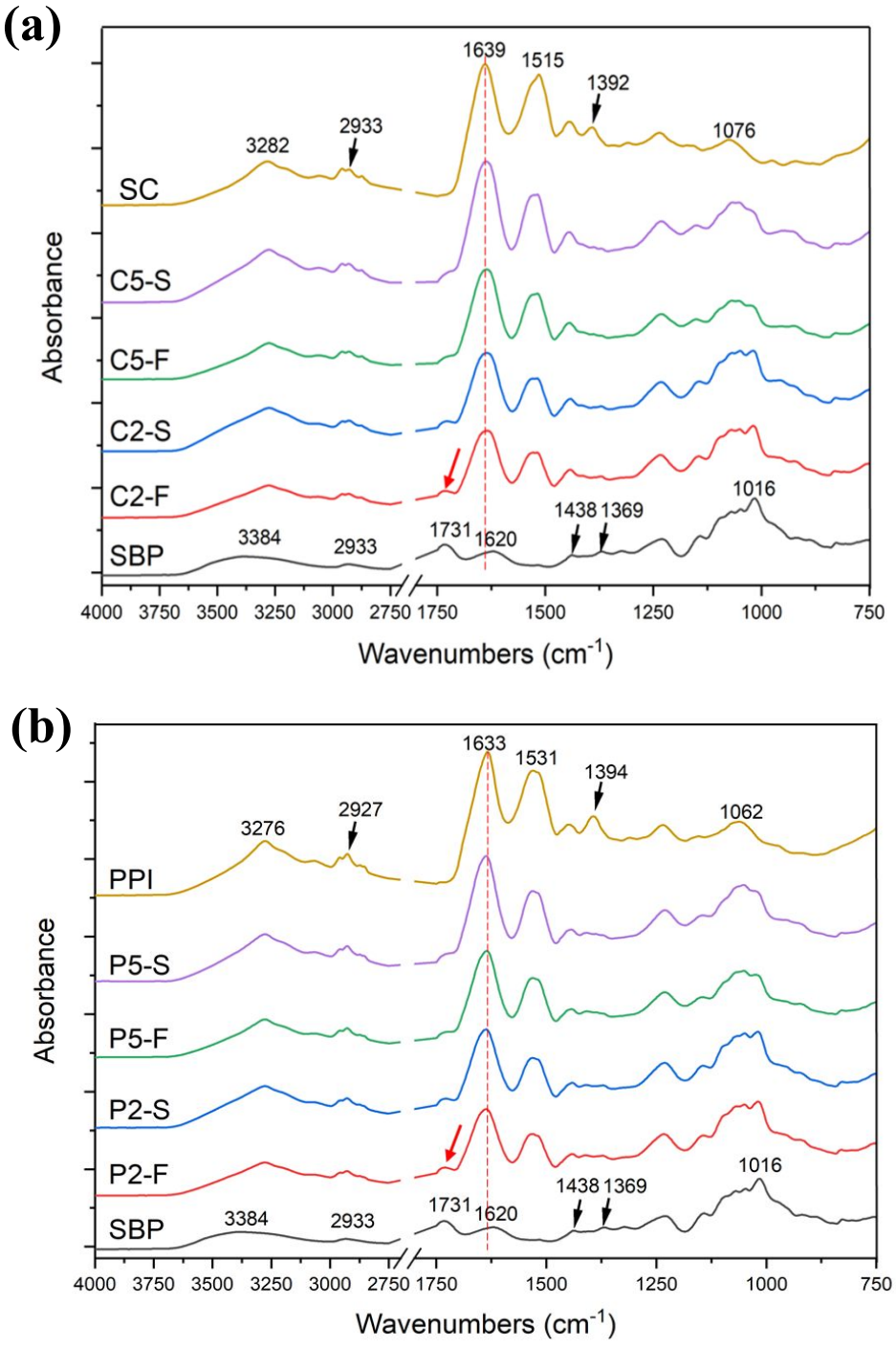

Fig. 3. FTIR spectra of *Lactobacillus rhamnosus* GG (LGG) encapsulated microcapsules by means of protein–SBP complex coacervates with different drying method (spray-drying and freeze-drying). (a) PPI–SBP complex coacervates; and (b) SC–SBP complex coacervates. The formulation and code of the samples are listed in Table S-1.

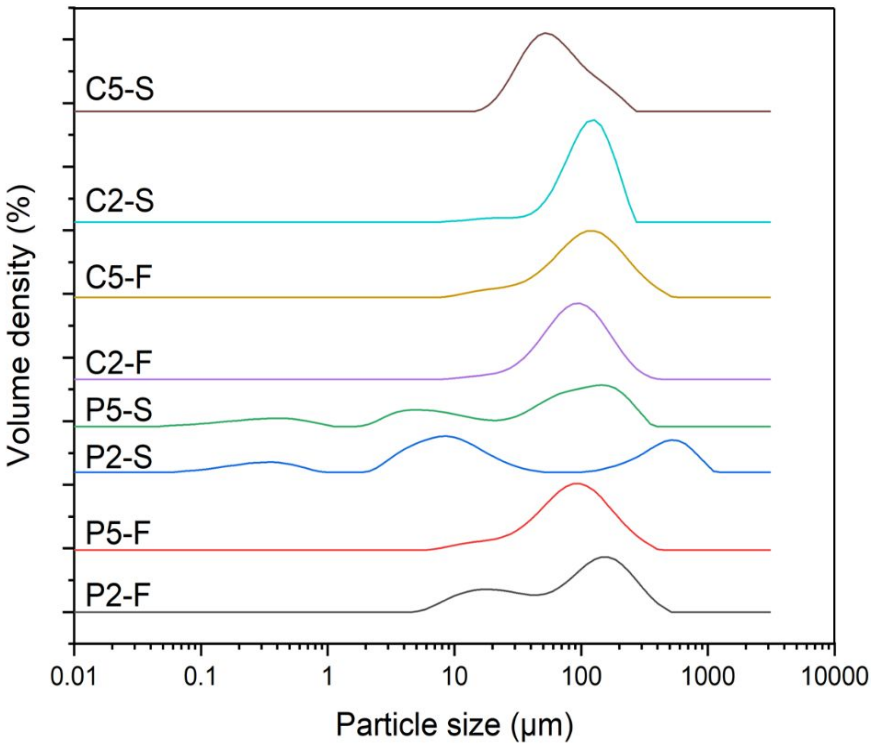

Fig. 4. Particle size distribution of LGG encapsulated spray-dried and freeze-dried microcapsules. The formulation, code and the particle size $D_{(50)}$ of the samples are listed in Table S-1.

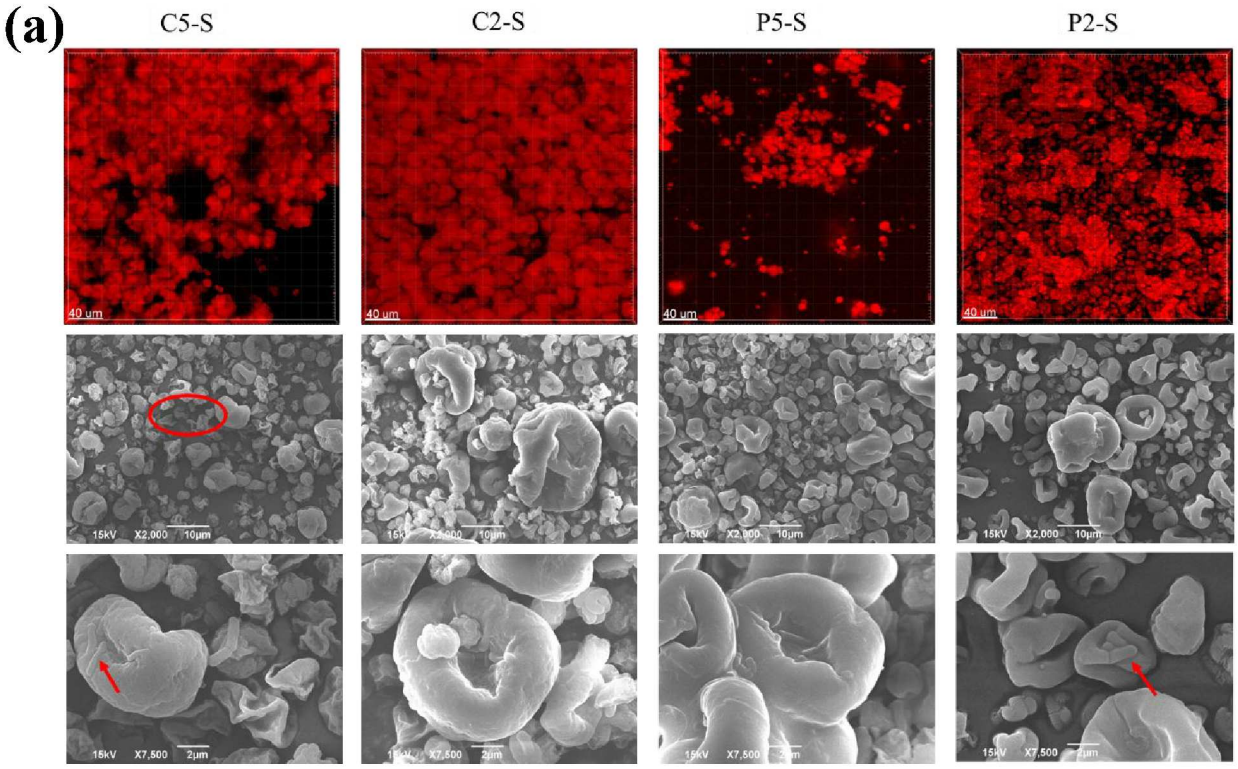
(a)
C5-S
C2-S
P5-S
P2-S
40 μm
15kV X2,000 10μm
15kV X7,500 2μm

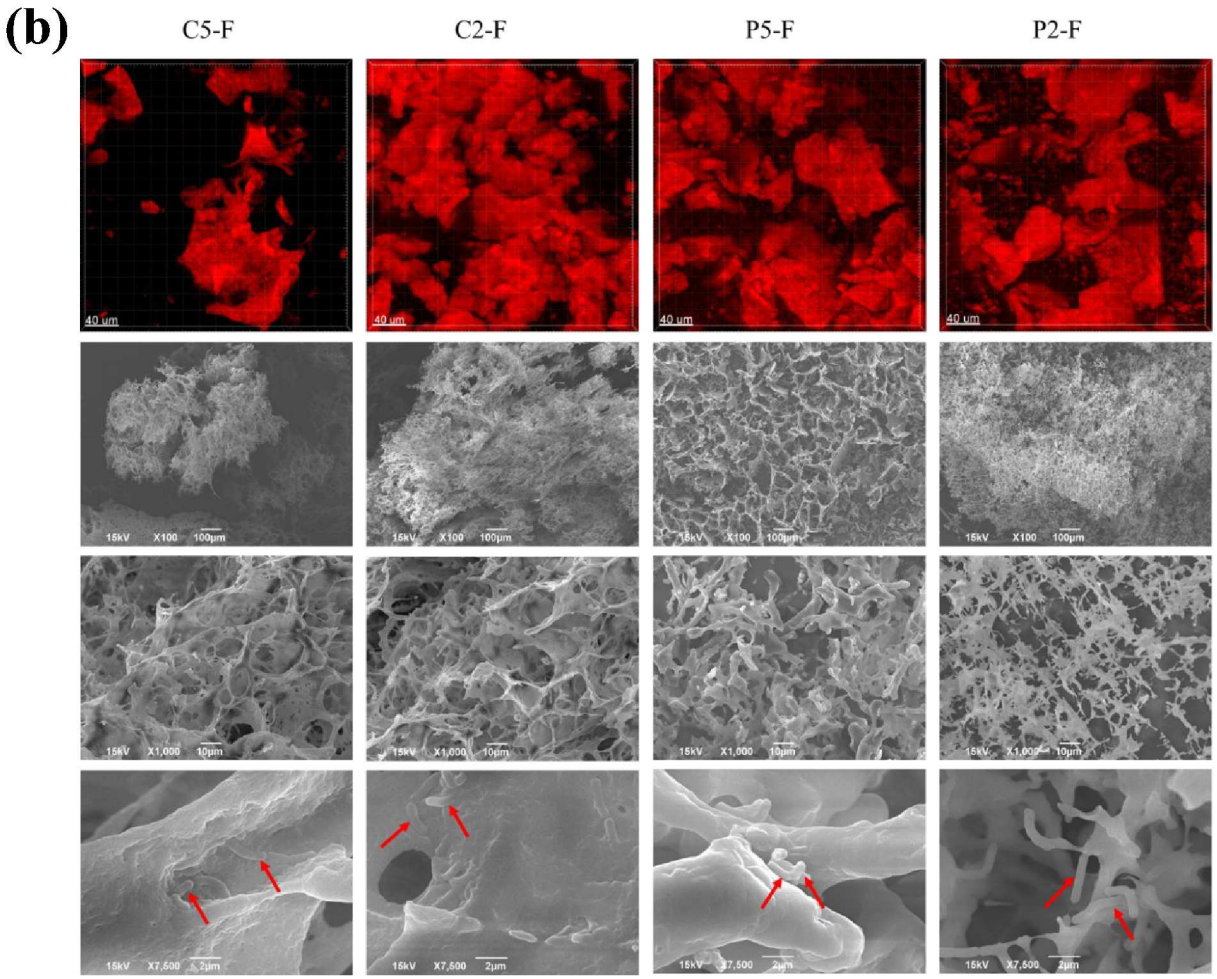

Fig. 5. The confocal laser scanning microscopy (CLSM) images (first row) and scanning electron microscopy (SEM) images under different magnifications of (a) LGG encapsulated spray-dried microcapsules; and (b) LGG encapsulated freeze-dried microcapsules. Protein was labeled as red color in CLSM images. Arrow indicated LGG cells, and the severely crumpled surface was marked by circle in SEM images. The formulation and code of samples are listed in Table S-1.

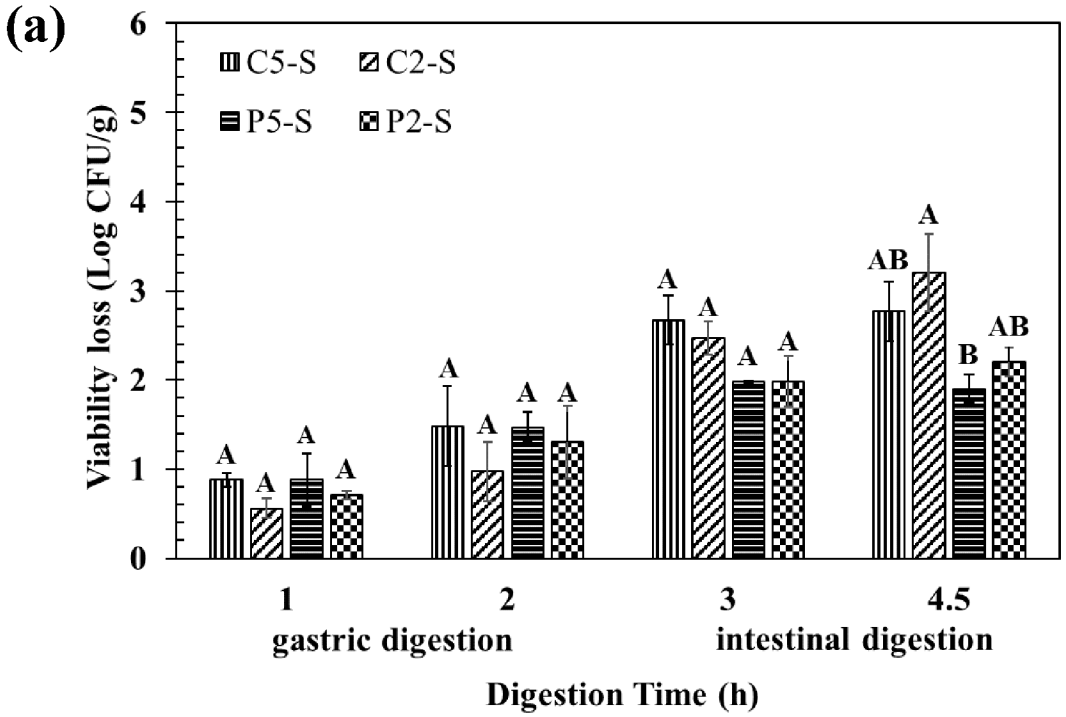
(a)
C5-S
C2-S
P5-S
P2-S
Viability loss (Log CFU/g)
0
1
2
3
4
5
6
A
A
A
A
A
A
A
A
A
A
AB
A
B
AB
1
2
3
4.5
gastric digestion
intestinal digestion
Digestion Time (h)

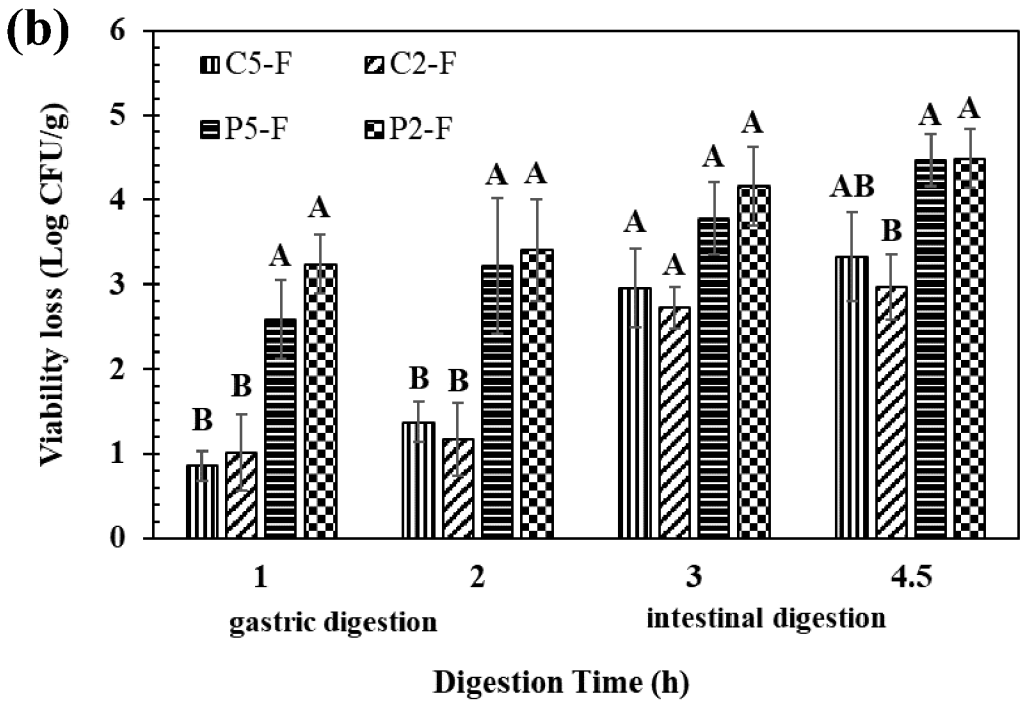
(b)
C5-F
C2-F
P5-F
P2-F
Viability loss (Log CFU/g)
0
1
2
3
4
5
6
B
B
A
A
B
B
A
A
A
A
A
A
AB
B
A
A
1
2
3
4.5
gastric digestion
intestinal digestion
Digestion Time (h)

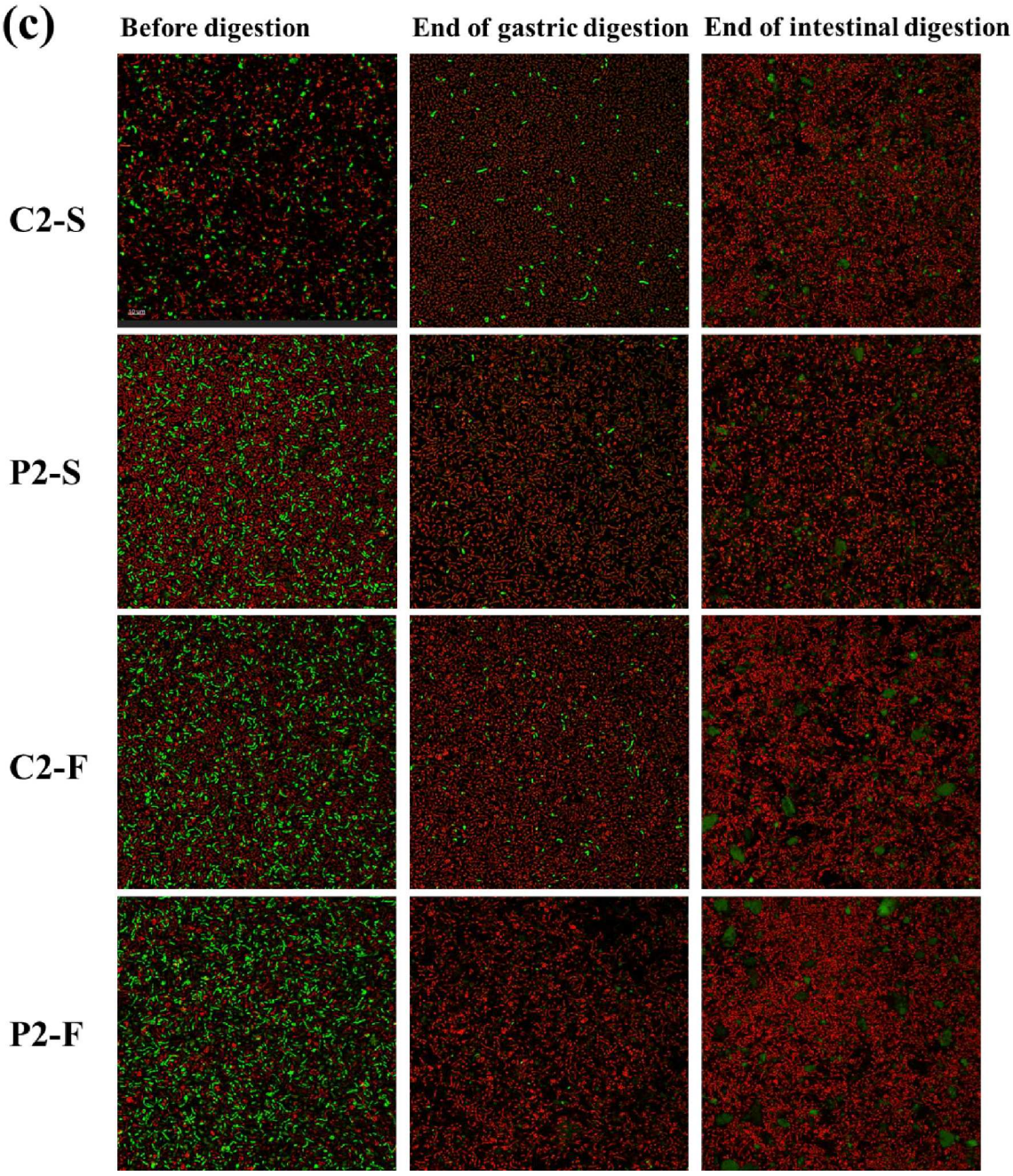

Fig. 6. Viability loss of LGG encapsulated in (a) spray-dried coacervates and (b) freeze-dried coacervates during simulated gastrointestinal digestion. (c) Live and dead cells observation under confocal during simulated gastrointestinal digestion. The values with different superscript letters within same time point are significantly different ($p < 0.05$).